

GCA Technical Report No. 65-6-N

PLANETARY PHYSICS X:  
TOTAL ABSORPTION CROSS SECTION OF  
ATOMIC OXYGEN BELOW  $910\text{\AA}$

R. B. Cairns  
James A. R. Samson

May 1965

Contract No. NASw-840

GCA CORPORATION  
GCA TECHNOLOGY DIVISION  
Bedford, Massachusetts

Prepared for  
National Aeronautics and Space Administration  
Headquarters  
Washington, D. C.

~~CONFIDENTIAL~~

## TABLE OF CONTENTS

<u>Title</u>	<u>Page</u>
SUMMARY	1
INTRODUCTION	1
EXPERIMENTAL	3
THE PRODUCTION OF ATOMIC OXYGEN	5
THE ATOMIC OXYGEN PHOTOABSORPTION CROSS SECTION	11
DISCUSSION OF RESULTS	15
REFERENCES	19
APPENDIX — TECHNIQUES FOR THE PRODUCTION OF A HIGH OXYGEN ATOM CONCENTRATION	21

## PLANETARY PHYSICS X:

### TOTAL ABSORPTION CROSS SECTION OF ATOMIC OXYGEN BELOW 910<sup>0</sup><sub>Å</sub>

By R. B. Cairns and James A. R. Samson

#### SUMMARY

The total absorption cross section of atomic oxygen has been measured in the wavelength range 910 - 504<sup>0</sup><sub>Å</sub>. The results are compared with existing theoretical computations. The source of oxygen atoms was a microwave discharge in a He-O<sub>2</sub> mixture. In addition to the oxygen atoms, excited oxygen molecules in the <sup>1</sup> $\Delta_g$  state and metastable He atoms were formed. The procedure taken to extract the oxygen atom cross section from those of the other neutral and excited species is given.

#### INTRODUCTION

For an improved understanding of the Earth's upper atmosphere it is necessary to know the photoionization cross section ( $\sigma_i$ ) and the photoabsorption cross section ( $\sigma$ ) of each of its component gases. Cross sections of the majority of the atmospheric gases have been measured; however, no experimental data exist for atomic oxygen which is a dominant constituent above 160 km. The photoionization cross section of atomic oxygen has been computed by Bates and Seaton [1]\*, Dalgarno and Parkinson [2] and most recently by Dalgarno et al. [3]. This paper describes an experimental determination of the total absorption cross section of atomic oxygen at wavelengths shorter than its ionization threshold, 910<sup>0</sup><sub>Å</sub>. The results are compared with theory.

---

\*Numbers in [ ] throughout text indicate reference numbers.

## EXPERIMENTAL

A major difficulty in the experiment was the production of oxygen in sufficient number free from excited atomic and molecular states. Atomic oxygen can be produced when molecular oxygen is passed through an electrical discharge where it is partially dissociated. The evidence in the literature concerning the state of the gas emerging from the discharge is conflicting. For example, Linnet and Marsden [4] have summarized work which suggested that the discharged gas consists mainly of ground state atoms and molecules. Fite and Brackmann [5] were unable to detect excited species in concentrations greater than 3%. However, Foner and Hudson [6] and subsequent workers detected excited molecular species in considerable quantities. Since the rates of deactivation of these species on various glass and metal surfaces are different, the state of the gas downstream from the discharge depends on the materials used in the construction of apparatus. For this reason minimum reliance has been placed on published work.

The first part of this paper describes the production of atomic oxygen and the experiments made to identify other species present. The second part of the paper describes the cross section measurements.

## THE PRODUCTION OF ATOMIC OXYGEN

The apparatus used is shown in Figure 1. The source of atomic oxygen was an electrodeless microwave discharge operating at a frequency of 2450 Mc/sec. The degree of dissociation of molecular oxygen was promoted with two known techniques. Firstly traces of water vapor were not removed and secondly the oxygen was mixed with helium: the ratio was approximately four parts of helium to one part of oxygen. The discharged gas flowed through a 30 cm long pyrex absorption cell, which was attached to the exit slit of a one-half meter Seya monochromator. A monochromatic photon beam passed axially through the cell and was detected by a windowless photomultiplier. The multiplier was maintained at a pressure of about  $10^{-5}$  mm Hg using a differential pumping section with 1 mm diameter holes drilled in its opposite faces to allow passage of the photon beam. With this geometry a wavelength bandpass of 1.8Å was obtained.

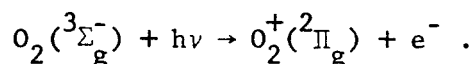
The number density of the oxygen atoms was measured at the midpoint of the absorption cell using the nitrogen dioxide titration technique [7,8]. The decay of atoms along the cell, due to wall and volume recombination, was determined by adding nitric oxide to the gas stream. Nitric oxide recombines with atomic oxygen emitting visible light. Since the decreasing intensity of the visible light along the cell gave a direct measurement of the oxygen atom concentration gradient, the total number of absorbing atoms could be determined.

With no gas discharge radiation with wavelengths shorter than 504Å was highly absorbed by He( $1^1S$ ) and at longer wavelengths the absorption was characteristic of molecular oxygen in its ground state  $O_2(^3\Sigma_g^-)$ . With the discharge switched on the absorption spectrum clearly showed the continued presence of both  $O_2(^3\Sigma_g^-)$  and He( $1^1S$ ). However at certain wavelengths longer than 910Å, the ionization onset of atomic oxygen in its ground  $^3P$  state, increased absorption was seen rather than the decrease expected since at these wavelengths the absorption cross section of  $O(^3P)$  is zero. Other species were present. In order to identify these species the absorption cell was converted to serve both as an absorption cell and an ionization chamber by placing within the cell two fine nickel wire ion collectors. Figures 2a - 2e show the results obtained with this modified cell.

Figure 2a shows the intensity of the light incident upon the absorbing gas measured as a function of wavelength.

Figure 2b shows the intensity of the light transmitted by the He- $O_2$  gas mixture when there was no discharge.

Figure 2c shows the ion current due to the photoionization process



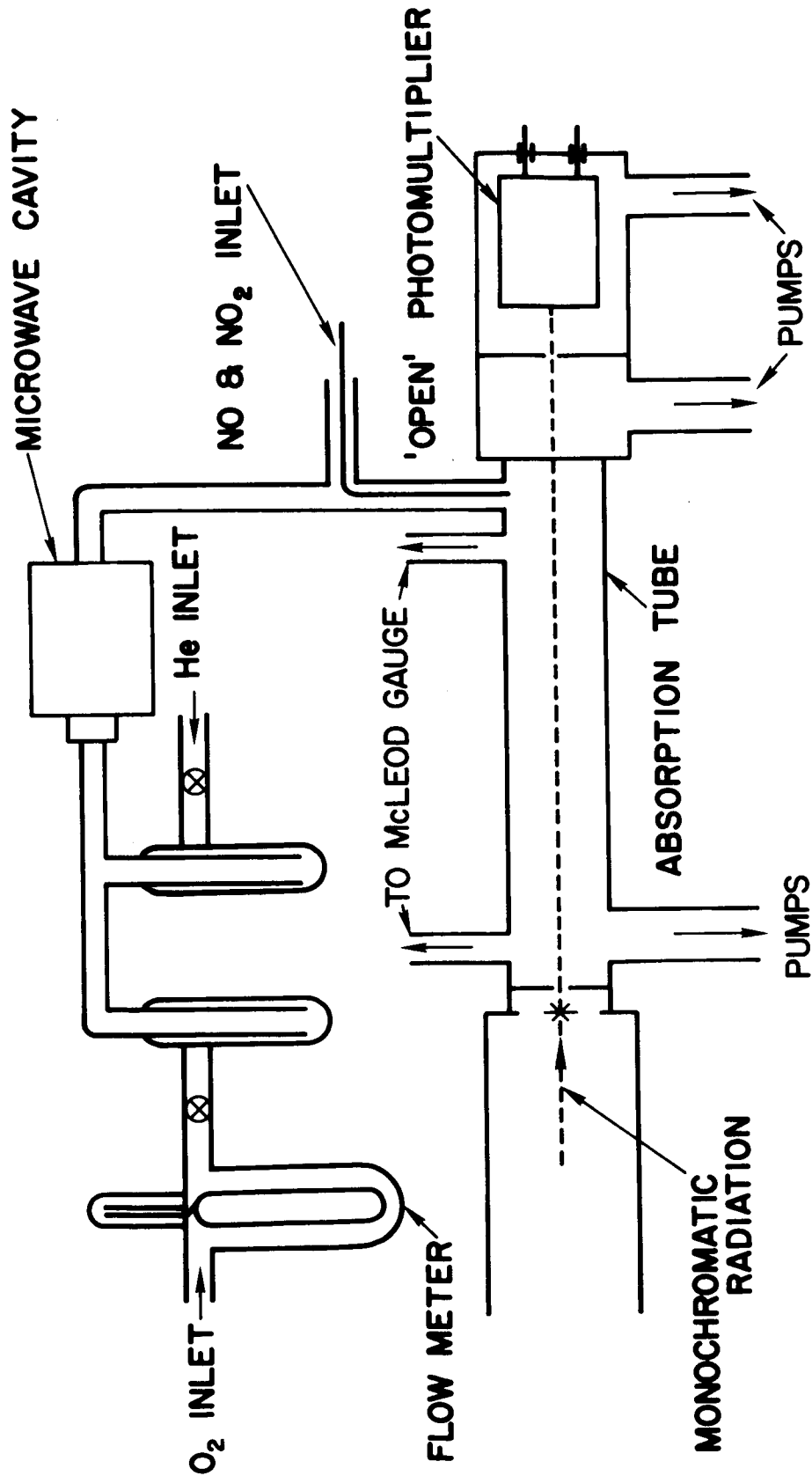


Figure 1. Schematic diagram of absorption cell, photon detector and gas inlet system.

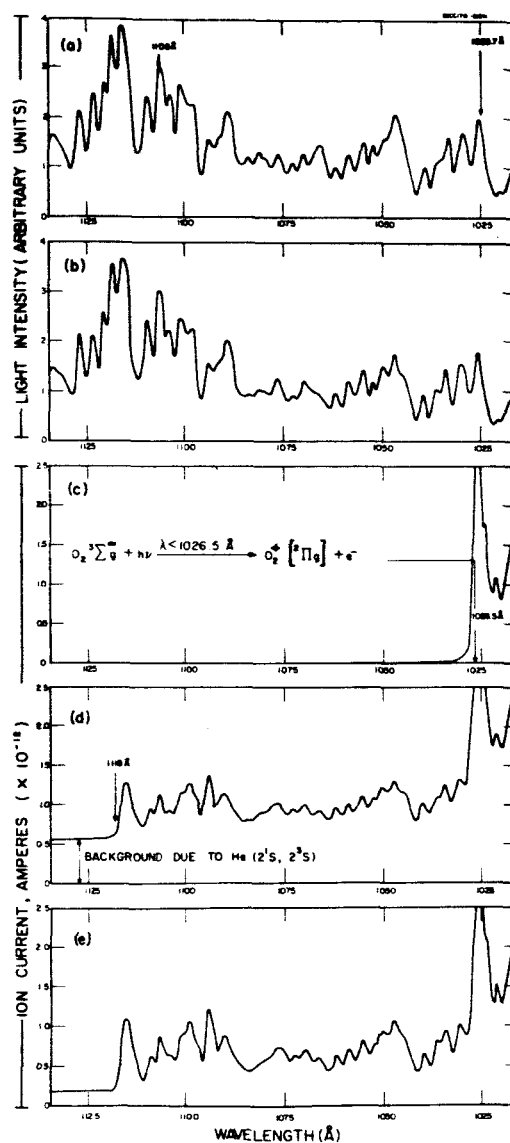


Figure 2. (a) The intensity of light incident upon the absorbing gas as a function of wavelength.

(b) The intensity of light transmitted by a  $He(1^1S) - O_2(^3\Sigma_g^-)$  gas mixture as a function of wavelength.

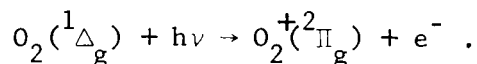
(c) The current due to the photoionization of  $O_2(^3\Sigma_g^-)$  as a function of wavelength.

(d) The current due to the photoionization of both  $O_2(^3\Sigma_g^-)$  and  $O_2(^1\Delta_g)$  as a function of wavelength.

(e) The current due to the photoionization of both  $O_2(^3\Sigma_g^-)$  and  $O_2(^1\Delta_g)$ , as a function of wavelength, when oxygen atoms have recombined on a mercuric oxide surface.

The conditions were as for 2b, i.e. there was no discharge. The photo-ionization threshold of  $O_2(^3\Sigma_g^-)$ <sup>9</sup> is indicated.

Figure 2d shows the ion current when the He- $O_2$  gas mixture was discharged. The ionization threshold was shifted to a longer wavelength indicating the presence of an additional species with an ionization potential  $0.99 \pm 0.04$  eV less than that of ground state  $O_2$ . This energy difference is equal to the energy separation of the  $^1\Delta_g$  and  $^3\Sigma_g^-$  states of  $O_2$ . Thus ionization at wavelengths shorter than 1118Å was at least partially due to the process



The conclusion that  $^1\Delta_g$  molecules were formed within the discharge agrees with the work of Foner and Hudson [6] who used electron impact techniques. At wavelengths longer than 1118Å, there remained an appreciable ion current. Since the magnitude of this current was independent of wavelength excited molecular states of  $O_2$  with energies greater than the  $^1\Delta_g$  state, for example the  $^3\Sigma_u^+$  and  $^1\Sigma_g^+$  states, could not have been present in measurable quantities. The constant current was ascribed to the ejection of electrons from the ion collectors by impacting metastable helium atoms. This was confirmed with ion collectors of different geometries. Account had to be taken of the fact that metastable helium atoms can be ionized in this wavelength region. However, the ion current was reduced by less than 5% when the photon beam was switched off showing that these metastables absorbed very little of the incident light.

The species identified in the discharged gas were, therefore,  $O_2(^3\Sigma_g^-)$ ,  $O_2(^1\Delta_g)$ ,  $O(^3P)$ , and metastable helium atoms. Oxygen atoms in the  $^1D$  and  $^1S$  states and ozone were assumed to be present in insufficient quantities to effect the cross section measurements.

To determine the oxygen atom cross section it was necessary to remove selectively either the oxygen atoms or the  $O_2(^1\Delta_g)$  molecules. Elias et al. [10] have reported a means of obtaining this discrimination: oxygen atoms recombine rapidly on a mercuric oxide surface but the  $O_2(^1\Delta_g)$  molecules are not deactivated. A glass tube coated with mercuric oxide was placed in the flow system. It could be positioned either up or downstream from the discharge. In the upstream position, the atom and metastable concentrations were unaffected. In the downstream position, the mercuric oxide removed 97% of the oxygen atoms. The ion chamber was used firstly to confirm that the mercuric oxide did not deactivate  $O_2(^1\Delta_g)$  molecules and secondly to indicate whether the oxygen atoms recombined to form ground state or excited oxygen molecules. Figure 2e shows the ion current measured with mercuric oxide downstream from the discharge. A comparison of Figures 2d and 2e shows that the mercuric oxide caused an increase in the  $O_2(^1\Delta_g)$  concentration but deactivated about 70% of the metastable helium atoms. A fraction of the oxygen atoms must have recombined to form the additional  $O_2(^1\Delta_g)$ . Measurable quantities of more highly excited molecular states were not detected in the ion chamber. (States with a lifetime of less than about  $1 \times 10^{-1}$  sec formed on



the mercuric oxide would not have reached the ion chamber.) At  $1108\text{\AA}$  where the attenuation of the photon beam by both  $\text{O}_2(^3\Sigma_g^-)$  and  $\text{O}_2(^1\Delta_g)$  was small (the absorption cross section of  $\text{O}_2(^3\Sigma_g^-)$  at this wavelength is  $\simeq .0074 \text{ Mb}^{11}$ ), the ratio of the ions produced before and after introduction of the mercuric oxide gave the ratio of the number densities of  $\text{O}_2(^1\Delta_g)$  molecules. For the pressure range used in these experiments the density of  $\text{O}_2(^1\Delta_g)$  molecules was increased  $20 \pm 4\%$  when the oxygen atoms were recombined on the mercuric oxide surface.

## THE ATOMIC OXYGEN PHOTOABSORPTION CROSS SECTION

The discharged gas contained  $O_2(^3\Sigma_g^-)$ ,  $O_2(^1\Delta_g)$ ,  $O(^3P)$ ,  $He(1^1S)$ , and  $[He(2^1S) - (2^3S)]$ . Helium  $1^1S$  atoms do not absorb at wavelengths longer than 504Å with the exception of the wavelengths corresponding to  $1^1S - m^1P$  transitions. The  $2^1S$  and  $2^3S$  metastable helium atoms absorb continuously at wavelengths shorter than 3245Å and 2610Å, respectively. Their absorption was, however, sufficiently weak to be neglected. Therefore a measurement of the oxygen atom photoabsorption cross section in the wavelength range 910Å to 504Å had to take account only of  $O_2(^3\Sigma_g^-)$ ,  $O_2(^1\Delta_g)$ , and  $O(^3P)$ .

An expression for the atomic cross section can be derived from the measured parameters using the Lambert-Beer Law.

With mercuric oxide upstream from the discharge, one obtains

$$I'_\nu = I_\nu^0 \exp -L[\sigma_\nu(O_2)n'(O_2) + \sigma_\nu(O_2^*)n'(O_2^*) + \sigma_\nu(O)n'(O)] , \quad (1)$$

where  $I_\nu^0$  is the intensity of the light, of frequency  $\nu$ , incident upon the absorbing gas (arbitrary units),

$I'_\nu$  is the intensity of the light, of frequency  $\nu$ , transmitted by the absorbing gas (arbitrary units),

$L$  is the length of the absorbing gas column (cm),

$\sigma_\nu(O_2)$ ,  $\sigma_\nu(O_2^*)$ , and  $\sigma_\nu(O)$  are the photoabsorption cross sections of  $O_2(^3\Sigma_g^-)$ ,  $O_2(^1\Delta_g)$ , and  $O(^3P)$ , respectively ( $\text{cm}^2$ ).

and  $n'(O_2)$ ,  $n'(O_2^*)$ , and  $n'(O)$  are the number densities of  $O_2(^3\Sigma_g^-)$ ,  $O_2(^1\Delta_g)$  and  $O(^3P)$ , respectively (particles per  $\text{cm}^3$ ).

With mercuric oxide downstream from the discharge,

$$I''_\nu = I_\nu^0 \exp -L[\sigma_\nu(O_2)n''(O_2) + \sigma_\nu(O_2^*)n''(O_2^*) + \sigma_\nu(O)n''(O)] . \quad (2)$$

The different superscripts used in Equations (1) and (2) denote changes in the magnitudes of  $I'_\nu$ ,  $n'(O_2)$ ,  $n'(O_2^*)$ , and  $n'(O)$ .

Since the quantity of molecular oxygen flowing per sec into the system remained constant,

$$N(O_2) = n'(O_2) + n'(O_2^*) + \frac{1}{2}n'(O) = n''(O_2) + n''(O_2^*) + \frac{1}{2}n''(O) \quad (3)$$

where  $N(O_2)$  was the number of oxygen molecules per cc when there was no discharge.

From Equations (1), (2), and (3)

$$\sigma(0) = \frac{1}{2}\sigma(O_2) - \frac{\left[ \frac{1}{L} \ln \frac{I'_v}{I''_v} + \frac{(n'(O_2^*) - n''(O_2^*))}{n''(O_2^*)} \left( \frac{1}{L} \ln \frac{I^o_v}{I''_v} - N(O_2)\sigma(O_2) \right) \right]}{\left[ (n'(0) - n''(0)) - n''(0) \frac{(n'(O_2^*) - n''(O_2^*))}{n''(O_2^*)} \right]} \quad (4)$$

An experiment previously described in this paper showed that the number density of  $O_2(^1\Delta_g)$  molecules increased by 20% in the presence of mercuric oxide, i.e.  $n''(O_2^*) \simeq 6/5 n'(O_2^*)$

therefore,

$$\frac{n'(O_2^*) - n''(O_2^*)}{n''(O_2^*)} = -\frac{1}{6} \quad (5)$$

Equations (4) and (5) give an expression for  $\sigma(0)$  which involves measured quantities only:  $I^o_v$ ,  $I'_v$ , and  $I''_v$  were measured with the windowless multiplier,  $n'(0)$  and  $n''(0)$  with the  $NO_2$  titration technique, and  $N(O_2)$  with a sensitive McLeod gauge. The effective length  $L$  of the absorbing gas column was assumed to equal the length of the absorption cell, i.e. no account was taken of both the viscous pressure drop and the pressure gradients at the ends of the cell. This assumption contributed to a total error in the determination of  $\sigma(O_2)$ , estimated from a comparison with more accurate data previously obtained [12], of less than 10%. (Under all conditions the calculated pressure difference between the ends of the cell due to viscous flow was less than 8% of the mean measured pressure.)

The estimated error in the determination of  $\sigma(0)$  was  $\pm 30\%$ . Values of this cross section are listed in Table I.

TABLE I  
ABSORPTION CROSS SECTION OF ATOMIC OXYGEN

$\lambda[\text{\AA}]$	$\sigma(O)[\text{cm}^2 \times 10^{-18}]$	$\lambda[\text{\AA}]$	$\sigma(O)[\text{cm}^2 \times 10^{-18}]$
508.434 A III } 508.595 A III }	13.3	725.542 A II	16.7
551.371 A VI	13.2	735.89 Ne I	14.3
584.331 He I	11.9	743.70 Ne I	7.6
585.754 A VII	12.3	758.677 O V } 759.440 O V } 760.229 O V } 760.445 O V } 761.130 O V } 762.001 O V }	8.3
624.617 O IV } 625.130 O IV } 625.852 O IV }	13.0	760.439 A IV	7.9
636.818 A III } 637.282 A III }	13.7	774.522 O V	7.6
683.278 A IV	11.8	779.821 O IV } 779.905 O IV }	11.1
684.996 N III } 685.513 N III } 685.816 N III } 686.335 N III }	17.3	822.159 A V	6.0
699.408 A IV } 700.277 A IV }	12.7	832.754 O II } 832.927 O III } 833.326 O II } 833.742 O III } 834.462 O II }	5.3
702.332 O III } 702.822 O III } 702.899 O III } 703.850 O III }	13.0	850.602	5.0
715.599 A V } 715.645 A V }	12.2	901.168 A IV } 901.804 A IV }	4.7

## DISCUSSION OF RESULTS

The measured total absorption cross section of atomic oxygen has been plotted in Figure 3 together with values of its ionization cross section obtained theoretically using both the dipole velocity and dipole length formulations [3]. Dalgarno *et al.* [3] favored the results given by the dipole velocity calculation since the iterative process involved converged more rapidly. In addition, the dipole velocity calculation was expected to be more accurate at short wavelengths [13].

The experimental points all lie above the preferred theoretical curve. The measured cross section at  $902\text{\AA}$ , close to the photoionization threshold, is about 50% higher than that calculated. The increases in cross section obtained theoretically at  $732\text{\AA}$  and  $665\text{\AA}$ , due respectively to the added possibilities of ionization to the  $^2\text{D}$  and  $^2\text{P}$  states of  $\text{O}^+$ , are not positively confirmed by experiment. It is possible that these edges exist, but are hidden by absorption in line series going to the two series limits 16.86 and 18.54 volts above the ground state of the oxygen atom. If an atom is excited to a discrete energy state lying above its lowest ionization potential, it can de-excite with the emission of radiation or, selection rules permitting, can undergo a radiationless transition to an adjoining continuum. In atomic oxygen both of these processes are possible. Thus at certain wavelengths less than  $910\text{\AA}$  all photons absorbed do not ionize atomic oxygen either by direct ionization or pre-ionization. At these wavelengths the total absorption cross section is greater than the ionization cross section. At wavelengths where pre-ionization occurs the absorption lines are broadened and, if accounted for, could greatly alter the computed photoionization cross section. These considerations may explain the differences, which are largest at  $780\text{\AA}$ ,  $736\text{\AA}$ ,  $725\text{\AA}$ , and  $686\text{\AA}$ , between the experimental and calculated cross sections.

At the  $584\text{\AA}$  He I line, prominent in the solar spectrum, the measured cross section is  $11.9 \times 10^{-18} \text{ cm}^2$ . This is in good agreement with the value given by Dalgarno and Parkinson [2] and subsequently used in discussions of the formation of the Earth's ionosphere.

In the X-ray region the ionization cross section of atomic oxygen has been assumed to equal  $\frac{1}{2}\sigma(\text{O}_2)$  [14]. This assumption cannot be arbitrarily extended to longer wavelengths. However  $\frac{1}{2}\sigma(\text{O}_2)$ , measured over the wavelength range 300 to  $200\text{\AA}$  shows close agreement with the dipole length calculation [3]; see Figure 4. Measurements of  $\sigma(\text{O}_2)$  in this region have been reported by several authors [15-17]. Excellent agreement was obtained with the work of Po Lee [17].

In addition to the absorption cross section of atomic oxygen the experiment described gave both the product  $n(\text{O}_2^*)\sigma(\text{O}_2^*)$  and information as to whether  $\sigma(\text{O}_2^*)$  was greater or less than  $\sigma(\text{O}_2)$ . A technique for measuring  $n(\text{O}_2^*)$  has been discussed by Elias *et al.* [10]. Thus the absorption cross section of the  $\text{O}_2(^1\Delta_g)$  molecule could be measured. Elias *et al.* [10] found, in agreement

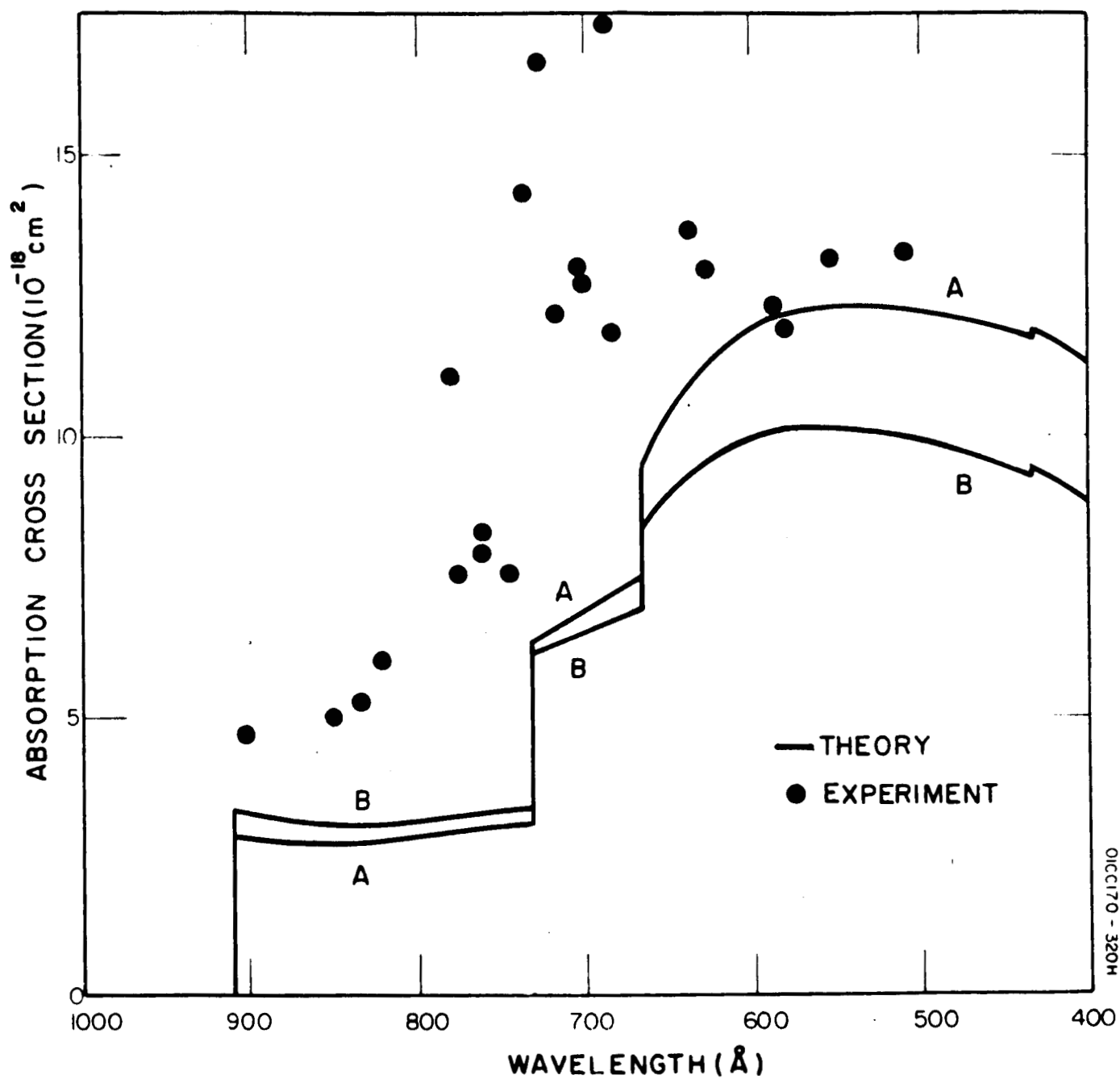


Figure 3. The absorption cross section of atomic oxygen,  $\lambda$  1000 —  $\lambda$  400 $\text{\AA}$ . Curves A and B were computed using the dipole length and dipole velocity formulations respectively. The experimental points have an estimated accuracy of  $\pm 30\%$ .

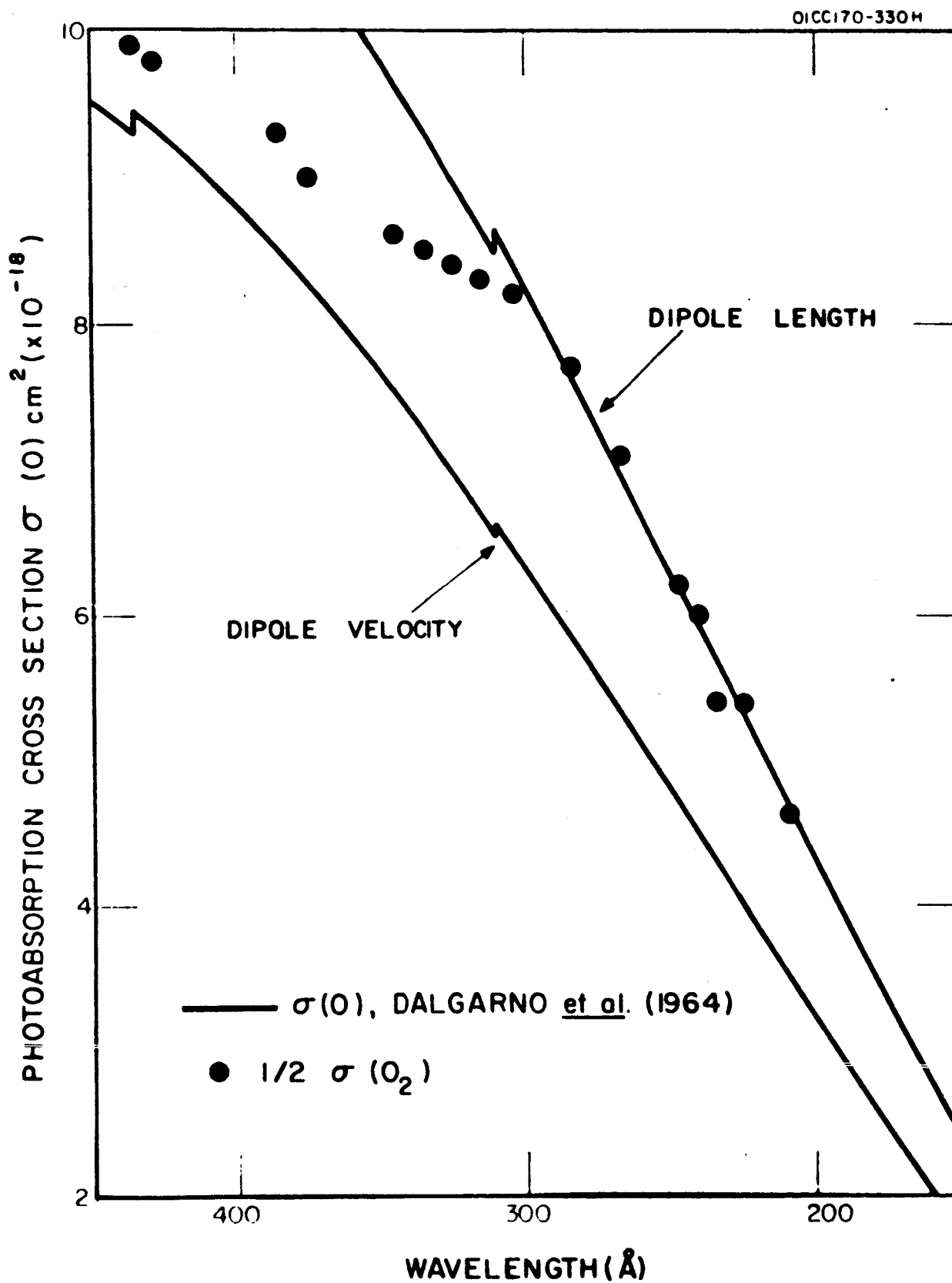


Figure 4. A comparison of the calculated photoionization cross section of atomic oxygen with one-half of the measured photoabsorption cross section of molecular oxygen.

with Foner and Hudson and Herron and Schiff [18], that about 10% of discharged oxygen is in the  $^1\Delta_g$  state. If this is so the fraction  $f$  of oxygen atoms recombining on the mercuric oxide surface to form  $O_2(^1\Delta_g)$  can be calculated since

$$n''(O_2^*) - n'(O_2^*) = \frac{1}{2}f[n'(O) - n''(O)] .$$

Using Equation (5), one obtains

$$n'(O_2^*) = \frac{5}{2} f [n'(O) - n''(O)] = \frac{1}{10} N(O_2) .$$

Therefore,

$$f = \frac{N(O_2)}{25[n'(O) - n''(O)]}$$

and when values of  $N(O_2)$ ,  $n'(O)$ , and  $n''(O)$  are substituted, one obtains  $f = 0.2$ .

A brief description of the technique used for the production of a high degree of dissociation of molecular oxygen is given in the Appendix.

#### ACKNOWLEDGMENT

The authors wish to thank Dr. H. I. Schiff for suggesting the use of mercuric oxide in these experiments.



## REFERENCES

1. Bates, D. R. and M. J. Seaton, *Mon. Not. Roy. Astron. Soc.*, 109, 698 (1949).
2. Dalgarno, A. and D. Parkinson, *J. Atmos. Terr. Phys.*, 18, 335 (1960).
3. Dalgarno, A., R. J. W. Henry and A. L. Stewart, *Plan. & Sp. Sci.*, 12, 235 (1964).
4. Linnett, J. W. and D. G. H. Marsden, *Proc. Roy. Soc. (London)*, A234, 489 (1956).
5. Fite, W. L. and R. T. Brackmann, *Phys. Rev.*, 113, 815 (1959).
6. Foner, S. N. and R. L. Hudson, *J. Chem. Phys.*, 25, 601 (1956).
7. Kaufman, F., *Proc. Roy. Soc.* A247, 123 (1958).
8. Kaufman, J. *Chem. Phys.*, 28, 352 (1958).
9. Watanabe, K. and F. F. Marmo, *J. Chem. Phys.*, 25, 965 (1956).
10. Elias, L., E. A. Ogryzlo and H. I. Schiff, *Can. J. Chem.*, 37, 1680 (1959).
11. Metzger, P. H. and G. R. Cook, *J. Quant. Spectrosc. Radiative Transfer*, 4, 107 (1964).
12. Samson, J. A. R. and R. B. Cairns, *J. Geoph. Res.*, 69, 4583 (1964).
13. Dalgarno, A. and J. T. Lewis, *Proc. Phys. Soc.*, A69, 285 (1956).
14. Compton, A. H. and S. K. Allison, *X-rays in Theory and Experiment*, D. VanNostrand Co., N. Y. (1935).
15. Aboud, A. A., J. P. Curtis, R. Mercure and W. A. Rense, *J. Opt. Soc. Am.*, 45, 767 (1955).
16. DeReilhac, L. and N. Damany-Astoin, *C. R. Acad. Sc. (Paris)*, 258, 519 (1964).
17. Lee, Po, *J. Opt. Soc. Am.*, 45, 703 (1955).
18. Herron, J. and H. Schiff, *Can. J. Chem.*, 36, 1159 (1958).

## APPENDIX

### TECHNIQUES FOR THE PRODUCTION OF A HIGH OXYGEN ATOM CONCENTRATION

The atoms were produced in a gas discharge. Three different power supplies were used:

- (1) an rf generator of high power but low frequency (output 20 kW at 450 kc/sec),
- (2) an rf generator of higher frequency but lower power (output 200 W at 10 Mc/sec), and
- (3) a microwave generator (output 120 W at 2450 Mc/sec).

The microwave generator was supplied with a tunable cavity. Most efficient coupling of the rf generators was obtained when the electrodes were of fine copper wire wrapped externally around the discharge tube and then painted over with "aquadag" to provide a large contacting surface. These three power supplies each produced nearly equal concentrations of oxygen atoms: with an  $O_2$  pressure of  $10^{-1}$  mm Hg, approximately 5% of the molecules were dissociated. The atom concentration increased with the output power of the generator. This increase was not linear. For example, when the output of the microwave generator was increased from 40 to 80% of full power the atom concentration increased less than 30%.

Two microwave and up to six rf discharges were run in parallel. No significant increase in the atom concentration was obtained.

An rf discharge maintained in series with and downstream from the microwave discharge removed all atoms produced in the microwave discharge. This has yet to be explained.

Over the limited pressure range employed in the experiments described in this report the percentage of oxygen molecules dissociated did not change appreciably. However at high pressures the percentage decreased.

The addition of a trace quantity of water vapor to the  $O_2$  is known to promote the production of oxygen atoms. The 5% dissociation quoted above was obtained using oxygen which had not been dried. Passing the oxygen through a liquid nitrogen cooled trap upstream from the discharge reduced the dissociation to about 1%. The number of excited  $^1\Delta_g$  oxygen molecules formed in the discharge was, however, nearly unaltered when the oxygen was dried.

The addition of a trace of  $H_2$  to the  $O_2$  increases the number of oxygen atoms produced: a 1% addition of  $H_2$  resulted in a three-fold increase in the atom density. However the rate of loss of atoms by volume recombination was also increased. This results in the atoms having a steep concentration gradient downstream from the discharge.

The technique finally employed to increase the atom density was the addition of a large quantity of the He to the O<sub>2</sub>. Owing to gas handling difficulties, the He/O<sub>2</sub> ratio did not exceed 5/1. The percentage dissociation reached 15%.